ChemPubSoc Europe

DOI: 10.1002/chem.201705410

CHEMISTRY
A European Journal
Full Paper

Spin Labels

Purine-Derived Nitroxides for Noncovalent Spin-Labeling of Abasic Sites in Duplex Nucleic Acids

Nilesh R. Kamble and Snorri Th. Sigurdsson*[a]

Abstract: A series of purine-based spin labels was prepared for noncovalent spin-labeling of abasic sites of duplex nucleic acids through hydrogen bonding to an orphan base on the opposing strand and π-stacking interactions with the flanking bases. Both 1,1,3,3-tetramethylisoindolin-2-yloxyl and 2,2,6,6-tetramethylpiperidine-1-oxyl (TEMPO) were conjugated to either the C2- or C6-position of the purines, yielding nitroxide derivatives of guanine, adenine, or 2,6-diaminopurine. The isoindoline-derived spin labels showed extensive or full binding to abasic sites in RNA duplexes, whereas the TEMPO-derived spin labels showed limited binding. An adenine-derived spin label (**5**) bound fully at low temperature to abasic sites in both DNA and RNA duplexes when paired with thymine and uracil, respectively, complementing the previously described guanine-derived spin label **Ǵ**, which binds efficiently opposite cytosine. Compound **Ǵ** was also shown to bind to abasic sites in DNA–RNA hybrids, either in the DNA- or the RNA-strand. **Ǵ** showed only a minor flanking-sequence effect upon binding to abasic sites in RNA. When the abasic site was placed close to the end of the RNA duplex, the affinity of the spin label **Ǵ** was reduced; full binding was observed at the fourth position from the duplex end. In summary, spin labels **5** and **Ǵ** showed full binding to abasic sites in both DNA and RNA duplexes and are promising spin labels for structural studies of nucleic acids by pulsed EPR methods.

Introduction

Electron paramagnetic resonance (EPR) spectroscopy is a biophysical technique that is used for the investigation of structure and dynamics of biomolecules, such as nucleic acids[1] and proteins.[1a,e,2] EPR studies require a small amount of sample (nmoles) and can be carried out under biologically relevant conditions. Continuous-wave (CW) EPR spectroscopy provides information about dynamics of specific sites through lineshape analysis of EPR spectra.[1d,3] CW-EPR has also been used for distance measurements between two spin centers in the range of 5–20 Å,[4] whereas pulsed EPR methods, such as pulsed electron–electron double resonance (PELDOR), also called double electron–electron resonance (DEER), and double quantum coherence (DQC), have been used for long-range distance measurements (20–100 Å).[1a,5] When used in conjunction with rigid spin labels, PELDOR can also provide valuable information about the conformational dynamics of nucleic acids.[6]

Most EPR studies of nucleic acids require attachment of paramagnetic groups at specific sites, referred to as site-directed spin labeling (SDSL).[1b,g,7] Stable aminoxyl radicals, commonly called nitroxides, are usually attached to the desired sites in the nucleic acid with covalent bonds.[7] For covalent spin-labeling, two main approaches have been used. The first method utilizes spin-labeled phosphoramidites as building blocks for automated chemical synthesis of the spin-labeled oligonucleotide either directly[8] or by using iodo-modified nucleobases for one-column coupling with spin labels.[9] However, the phosphoramidite approach usually requires a significant synthetic effort and the reagents used for oligonucleotide synthesis can partially reduce the nitroxide spin labels.[10] Post-synthetic labeling is another approach for covalent labeling, wherein a spin-labeling reagent is incubated with oligonucleotides that contain a uniquely reactive site.[11] Post-synthetic modification usually requires less synthetic effort than the phosphoramidite approach and can often be performed with commercially available reagents. However, post-synthetic labeling can result in side reactions and incomplete labeling.

Noncovalent spin-labeling of nucleic acids utilizes binding through van der Waals interactions, hydrogen bonding, and π-stacking interactions. Spin-labeled intercalators and groove binders can bind to nucleic acids noncovalently, but lack the sequence specificity that is required for most EPR studies.[12] There are a few examples of small molecules that bind noncovalently to specific sites of nucleic acids. Guanine–guanine mismatch-binding ligands carrying spin labels have been used to bind to predetermined sites of nucleic acids.[13] Abasic sites in duplex nucleic acids have also been used as binding sites for spectroscopic labels. For example, fluorescent compounds that bind to abasic sites have been developed by Teramae and coworkers for detection of single-nucleotide polymorphisms in DNAs.[14] Lhomme et al. used adenine–acridine conjugates for noncovalent spin-labeling of a DNA duplex containing an

[a] N. R. Kamble, Prof. S. Th. Sigurdsson
University of Iceland, Department of Chemistry
Science Institute, Dunhaga 3, 107 Reykjavik (Iceland)
E-mail: snorrisi@hi.is

Supporting information and the ORCID identification number for the author of this article can be found under https://doi.org/10.1002/chem.201705410.

© 2018 Wiley-VCH Verlag GmbH & Co. KGaA, Weinheim

abasic site in which the adenine bound to an abasic site and the acridine carrying the nitroxide spin label intercalated into the DNA duplex.[15]

We have previously used abasic sites in nucleic acids for noncovalent and site-directed spin labeling using pyrimidine-derived spin labels.[16] The spin label **ç** (Figure 1), which is an

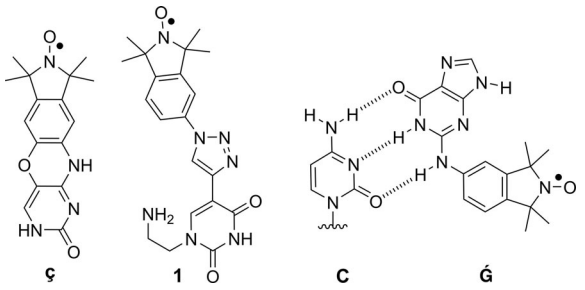

Figure 1. Structures of the spin label **ç** (left) and the triazole linked-nitroxide spin label **1** (middle). Proposed base-pairing of spin label **Ǵ** with **C** (right) at an abasic site in duplex nucleic acids.

analogue of cytosine (C), was found to bind specifically to abasic sites in duplex DNA opposite guanine (G).[16a] This label has been used for determination of distance as well as relative orientation between two spin labels in duplex DNA and in DNA–protein complexes.[17] However, the binding of **ç** was highly flanking-sequence dependent, showing full binding to only a few sequences. Moreover, **ç** showed only partial binding to an abasic site of an RNA duplex.[16c] A series of pyrimidine-derived nitroxides was subsequently prepared and screened for binding to both DNA and RNA duplexes.[16c] Only triazole-linked nitroxide **1** (Figure 1) showed complete binding to abasic sites in RNA, but it was not a useful spin label due to extensive nonspecific binding.[16c]

Given the limitations of the pyrimidine-based spin labels for noncovalent binding, we turned our attention to purine-derived nitroxides, because purines have a larger area for stacking interactions than pyrimidines. Recently, we reported the semi-flexible **Ǵ** (G-spin, Figure 1),[18] which is a conjugate of guanine and an isoindoline-derived nitroxide radical. The spin label **Ǵ** was found to bind specifically to abasic sites in DNA duplexes at low temperatures when paired with C as an orphan base on the opposite strand. More importantly, **Ǵ** was found to bind with much higher affinity to RNA, providing for the first time, a spin label that bound effectively to specific sites in RNA through noncovalent interactions.[18]

To further explore the use of purine-derived nitroxides for noncovalent spin-labeling of abasic sites in duplex DNA and RNA, we have prepared five new spin labels (**2**–**6**, Figure 2). The isoindoline-derived spin labels showed good binding affinity and specificity to both DNA and RNA duplexes containing an abasic site but the 2,2,6,6-tetramethylpiperidine-1-oxyl (TEMPO) derived spin labels bound poorly or not at all. Adenine (A)-derivative **5** bound fully to an abasic site in duplex RNA, providing the first nitroxide for noncovalent labeling of abasic sites opposite uridine (U). **Ǵ** can be used as a spin label for abasic sites in DNA–RNA hybrids, although it binds with

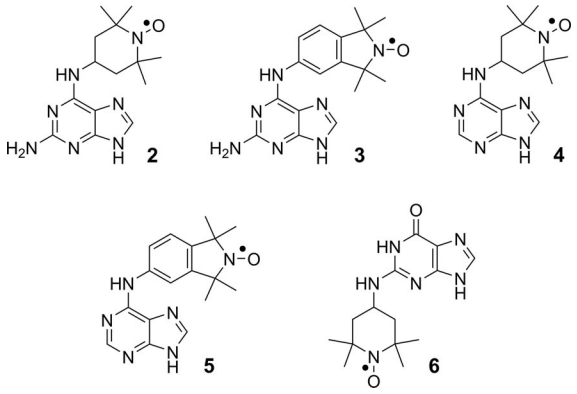

Figure 2. Structures of purine-derived spin labels **2**–**6**.

less affinity than to abasic sites in RNA. We also found that there is a minimal flanking-sequence dependence of **Ǵ** binding to abasic sites in RNA and that abasic sites need to be at least three base pairs away from the duplex end for complete binding.

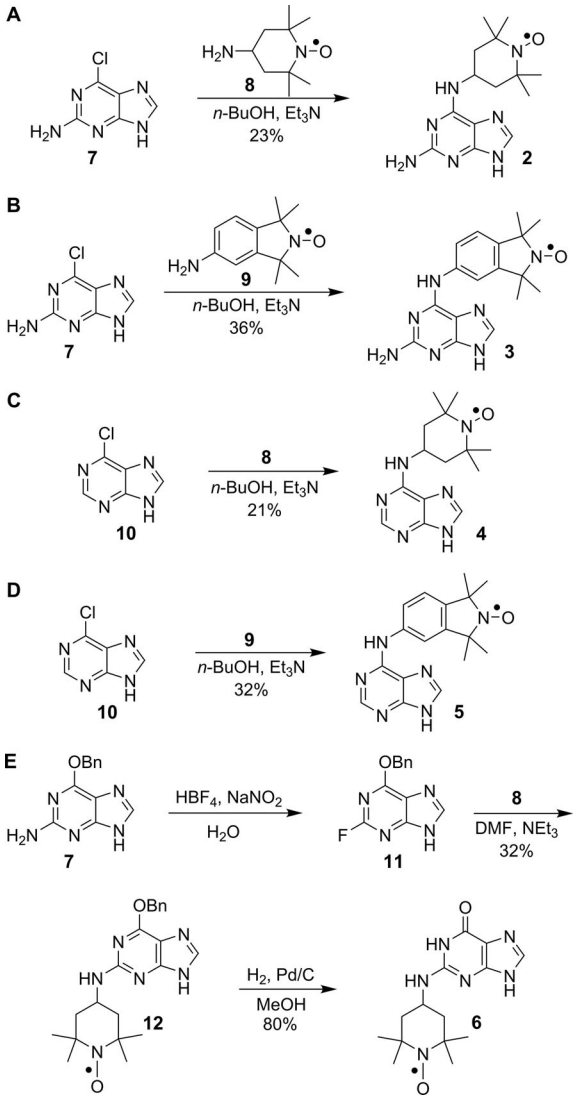

Scheme 1. Synthetic schemes for spin labels **2**–**6**.

© 2018 Wiley-VCH Verlag GmbH & Co. KGaA, Weinheim

Results and Discussion

The new purine-derived spin labels (Figure 2) contain nitroxides at either the C2- or the C6-position, affording either adenine-, guanine-, or 2,6-diaminopurine-derived spin labels. Two different nitroxides, 2,2,6,6-tetramethylpiperidine-1-oxyl (TEMPO) and 1,1,3,3-tetramethylisoindolin-2-yloxyl, were conjugated to the purines. Assuming Watson–Crick pairing to either U or C on the opposite strand, guanine-derived compounds **6** and **Ǵ** were expected to direct the nitroxide into the minor groove, whereas the 6-amino modified adenine and 2,6-diamino purine spin labels **2**–**5** would project the label into the major groove.

Syntheses of purine-derived spin labels

The spin labels were synthesized from readily available halogen-derived purines through direct nucleophilic displacement reactions. Commercially available 2-amino-6-chloropurine (**7**) was heated with either 4-amino-TEMPO (**8**) or isoindoline nitroxide **9**[19] to obtain 2,6-diamino purine derivatives **2** and **3**, respectively (Scheme 1 A and B). 6-Chloropurine (**10**) was reacted with **8** or **9** under similar conditions to give the corresponding spin-labeled adenine derivatives **4** and **5** (Scheme 1 C and D). For the synthesis of the guanine-derived TEMPO derivative **6**, we first attempted a reaction between **8** and 2-bromohypoxanthine in *N*,*N*-dimethylformamide (DMF) in the presence of triethylamine, but this resulted in the formation of a complex mixture of products (data not shown). Hence, the following sequence of reactions was used instead. 2-Amino-6-benzyloxy purine[20] (**7**) was reacted with sodium nitrite in the presence of tetrafluoroboric acid[21] to yield 2-fluoro-6-benzyloxypurine[20] (**11**) (Scheme 1 E). Compound **11** was subsequently reacted with 4-amino-TEMPO (**8**) to give **12** in moderate yield, which, upon debenzylation, gave the target compound **6** in excellent yield.

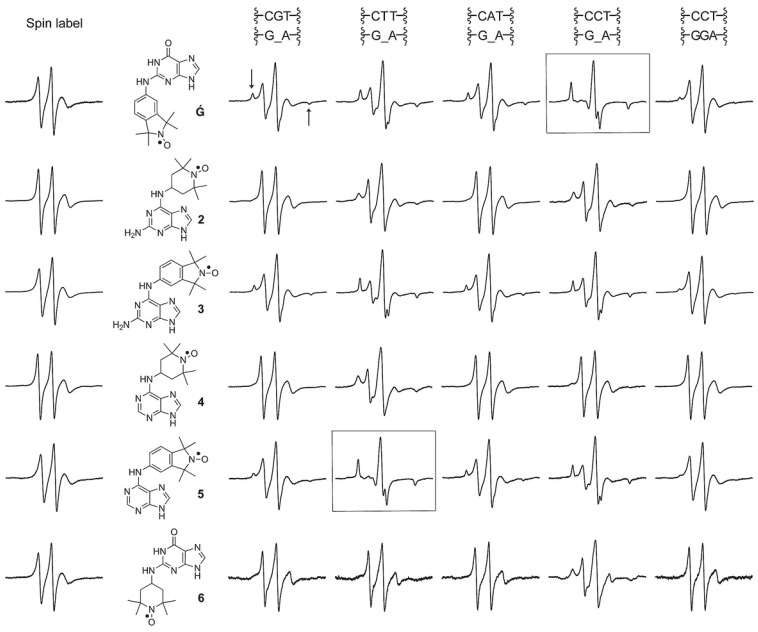

Figure 3. Binding of spin labels to abasic sites in DNA duplexes. EPR spectra of the spin labels are shown on the far left and EPR spectra of the labels in the presence of an unmodified DNA on the far right. The central four columns of EPR spectra show the spin-label in the presence of DNA duplexes containing an abasic site (denoted by "_") opposite the orphan bases G, T, A, and C. Only a part of the construct is shown on top; the complete DNA sequence is 5′-d(GACCTCG_ATCGTG)-3′·5′-d(CACGATXCGAGGTC)-3′, where X represents the orphan base (G, T, A, or C). The arrows by the spectra in the top left corner identify a slow-moving component in the EPR spectra, which indicates binding of a spin label to the nucleic acid. EPR spectra inside the black boxes showed almost fully bound **Ǵ** and **5** to the abasic site of a DNA duplex opposite C and T, respectively. EPR spectra of the spin labels (200 μM) in the presence of DNA duplexes (400 μM) were recorded in phosphate buffer (10 mM $NaHPO_4$, 100 mM NaCl, 0.1 mM Na_2EDTA, pH 7.0) containing 30% ethylene glycol and 2% DMSO at −30 °C. The spectra were phase-corrected and aligned with respect to the height of the central peak.

Binding of the spin labels to abasic sites in duplex DNA

The extent of binding and binding specificity of spin labels **2**–**6** to abasic sites in DNA duplexes were determined by EPR spectroscopy. Each spin label was incubated with a 14-mer duplex DNA containing G, T, A, or C as the orphan base at −30 °C (Figure 3). The EPR spectrum of each spin label (Figure 3, far left column) showed comparatively narrow lines, because of the fast tumbling of the radical in solution. In the presence of the DNA duplexes containing an abasic site, the appearance of a slow moving component in the spectrum (arrows in the top left spectrum) indicated binding of the spin label to the DNA. All the spin labels showed some binding affinity towards at least one DNA duplex. Two spectra indicated nearly full binding (>98%) to the abasic site (Figure 3, spectra in boxes), for previously reported spin label **Ǵ** opposite C and adenine-derived spin label **5** opposite thymine (T). The TEMPO derivatives **2**, **4**, and **6** showed very poor binding, whereas the 2,6-diaminopurine derivative **3** showed little to moderate binding (18–64%) to the abasic sites of the DNA duplexes. Notably, all the isoindoline-derived spin labels bind most extensively to an orphan base that can form a Watson–Crick base pair. However, extensive binding was observed to the other pyrimidine for these labels. This holds especially true for the 2,6-diaminopurine derivative **3**, because it binds to a somewhat similar extent to abasic sites with C (49%) and T (64%). For all the spin labels, there is considerably less binding to an abasic site containing a purine orphan base. To verify that the spin labels bind to the abasic site specifically, they were individually mixed with an unmodified 14-mer DNA duplex (Figure 3, far right column). Isoindoline-derived spin labels **Ǵ**, **3**, and **5** showed very minor levels of nonspecific binding (<3%).

Binding of the spin labels to abasic sites in duplex RNA

The extent of binding of the spin labels to abasic sites in RNA duplexes was also investigated (Figure 4). Here, the TEMPO-derived spin labels **4** and **6** also showed very limited binding (>30%) except for the 2,6-diamino derivative **2**, which showed extensive binding opposite C (87%). The isoindoline-derived spin labels **Ǵ**, **3**, and **5** had higher affinity to the abasic sites in

© 2018 Wiley-VCH Verlag GmbH & Co. KGaA, Weinheim

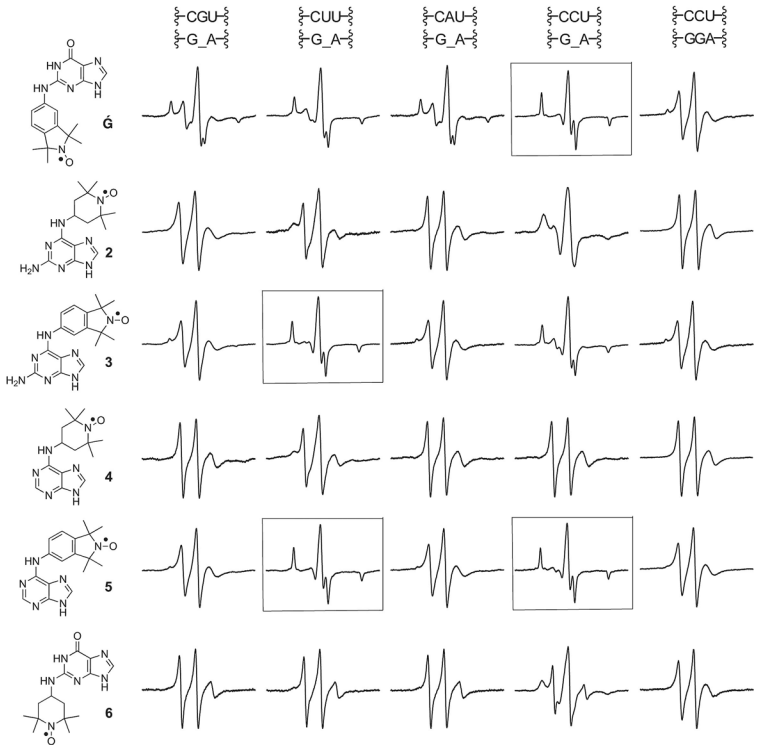

Figure 4. Binding of spin labels to abasic sites in RNA duplexes. EPR spectra of spin labels in the presence of an unmodified RNA are shown on the far right. The central four columns of the EPR spectra show the spin labels in the presence of RNAs containing an abasic site (denoted by "_") opposite the orphan bases G, U, A, and C. Only a part of construct is shown on top; the complete RNA sequence is 5′-GACCUCG_AUCGUG-3′·5′-CACGAUXCGAGGUC-3′, where X represents the orphan base (G, U, A, or C). EPR spectra inside the black boxes indicate full or nearly full binding. EPR spectra of the spin labels (200 μM) in the presence of RNA duplexes (400 μM) were recorded in phosphate buffer (10 mM $NaHPO_4$, 100 mM NaCl, 0.1 mM Na_2EDTA, pH 7.0) containing 30% ethylene glycol and 2% DMSO at −30 °C.

RNA duplexes than in DNA duplexes, showing full or nearly full binding to at least one sequence (Figure 4, black boxes). **Ġ** bound to an abasic site opposite C, 2,6-diamino purine **3** opposite U, whereas adenine derivative **5** bound opposite both pyrimidines, although it bound slightly better to U. All these spin labels show the best binding to abasic sites that contain an orphan base that can form Watson–Crick base pairs with the spin label. As was observed for DNA, the isoindoline-derived spin labels show extensive binding to abasic sites in RNA that contain either of the pyrimidine orphan bases. In particular, the adenine-derivative **5** binds almost fully (>98%) when paired with C. Combined with the fact that these spin labels have limited or no binding to abasic sites containing purines as the orphan base, it is clear that the shape/size of the binding pocket has a large effect on the specificity of binding.

To obtain information about the relative affinities of the isoindoline-derived spin labels **Ġ**, **3**, and **5**, the temperature dependence of their binding was investigated (Figure 5). Spin label **Ġ** was by far the best binder, with extensive binding being observed even at 20 °C (>95%, $K_d = 6.15 \times 10^{-6}$ M)[16a] at which temperature spin labels **3** and **5** showed nearly no binding.

Binding of the spin labels to abasic sites in DNA–RNA hybrids

DNA–RNA hybrids are heterogeneous nucleic acids and key intermediates in many important biological processes.[22] These hybrids are recognized by RNase H and have been used for biomedical technologies such as antisense therapies.[22c,23] Structures of several hybrids have been characterized using nuclear magnetic resonance (NMR) spectroscopy[24] and X-ray crystallography[25] and shown to be in an A-form duplex. Spin labeling of DNA–RNA hybrid duplexes have, to our knowledge, not been explored before. Given the extensive binding of the spin label **Ġ** to abasic sites in RNA, we selected it to probe its binding to abasic sites in DNA–RNA duplexes.

To evaluate the binding affinity of **Ġ** to the abasic site of DNA–RNA duplexes, two 14-mer duplexes were prepared. The first duplex contained an abasic site in the DNA strand (**DNA-RNA I**) and in the second duplex, the abasic site was placed in

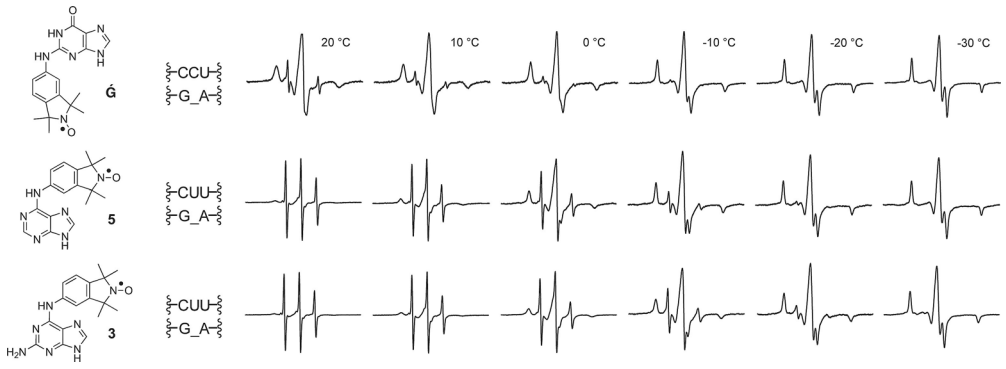

Figure 5. EPR spectra of the spin labels in the presence of an RNA duplex containing an abasic site at different temperatures. Only a part of construct is shown; the complete RNA sequence is 5′-GACCUCG_AUCGUG-3′·5′-CACGAUXCGAGGUC-3′; the abasic site (denoted by "_") and X represents orphan base C or U. EPR spectra of the spin labels (200 μM) in the presence of RNA duplexes (400 μM) were recorded in phosphate buffer (10 mM $NaHPO_4$, 100 mM NaCl, 0.1 mM Na_2EDTA, pH 7.0) containing 30% ethylene glycol and 2% DMSO.

© 2018 Wiley-VCH Verlag GmbH & Co. KGaA, Weinheim

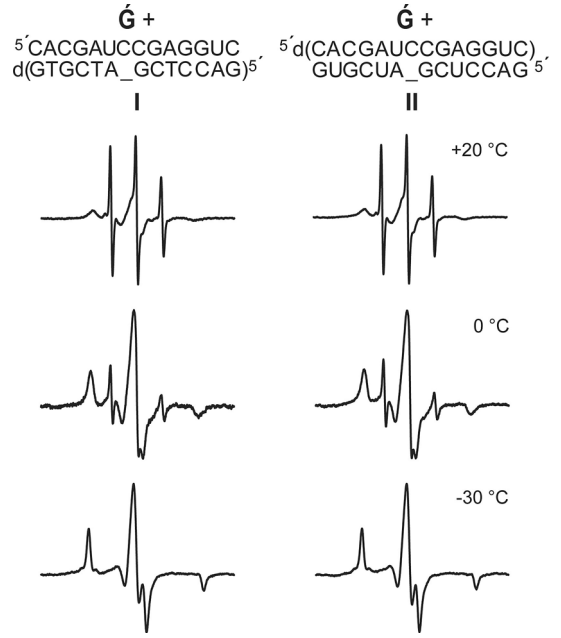

Figure 6. Binding of **Ġ** to an abasic site of DNA–RNA hybrid duplexes. The DNA–RNA **I** contained an abasic site in the DNA strand (left column), whereas the DNA–RNA **II** contained an abasic site in the RNA strand (right column) and the abasic sites are denoted by "_". EPR spectra of **Ġ** (200 μM) in the presence of DNA–RNA hybrid (400 μM) were recorded in phosphate buffer (10 mM $NaHPO_4$, 100 mM NaCl, 0.1 mM Na_2EDTA, pH 7.0) containing 30% ethylene glycol and 2% DMSO.

the RNA strand (**DNA-RNA II**). Figure 6 shows that **Ġ** bound fully to both hybrid duplexes at −30 °C, extensive binding (45–50%) was even observed at 0 °C. However, increasing the temperature to 20 °C resulted in almost complete loss of binding. We determined the binding affinities of **Ġ** to all the duplexes (DNA–DNA, RNA–RNA, and DNA–RNA) at 0 °C, where the abasic site was opposite C (see the Supporting Information Figure S1). **Ġ** had the highest affinity to the RNA duplex ($K_d = 1.46 \times 10^{-7}$ M), the second highest to the DNA–RNA ($K_d = 9.75 \times 10^{-7}$ M) and the lowest affinity to the DNA duplex ($K_d = 60.17 \times 10^{-7}$ M). Thus, the binding affinity of **Ġ** decreased sixfold when bound to DNA–RNA hybrids and 41-fold when it was bound to the DNA duplex at 0 °C, compared with the RNA duplex.

Effect of structural changes in RNA duplexes on binding of Ġ

Three main factors contribute to spin-label binding to an abasic site. First, hydrogen bonding of the spin-label base to the orphan base on the opposing strand, as described above. Second, the identity of the bases flanking the abasic site will affect the stacking interaction with the spin label. Third, placement of the abasic site close to the end of the duplex might compromise the structural integrity of the abasic binding site, because terminal base pairs are more dynamic than the central base pairs.[26] We decided to investigate the latter two factors in RNA using the spin label with the highest affinity (**Ġ**).

To probe the effect of the location of the abasic site relative to the duplex end on spin-label binding, four different 14-mer RNA duplexes (**III–VI**, Figure 7) were prepared, such that the position of the abasic site was moved one base pair at a time from the 5′-end towards the center of the duplex. Quite remarkably, **Ġ** showed extensive binding (77% at −30 °C) when

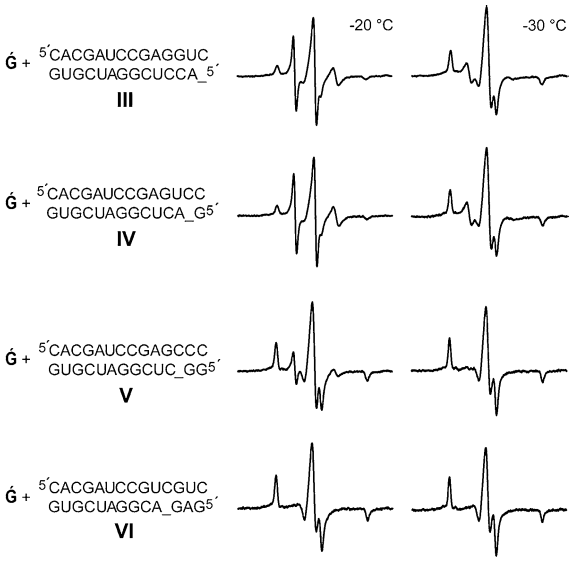

Figure 7. Binding of **Ġ** (200 μM) to RNA duplexes III–VI (400 μM) containing abasic sites (denoted by "_"), where the location of the abasic site is moving from the 5′-end to the center of the duplex. All EPR spectra were recorded in phosphate buffer (10 mM $NaHPO_4$, 100 mM NaCl, 0.1 mM Na_2EDTA, pH 7.0) containing 30% ethylene glycol and 2% DMSO.

a single C-overhang was placed at the end of the RNA duplex (**III**), similar to the degree of binding to an abasic site placed one base pair away from the end of the duplex (**IV**). When the abasic site was placed at the third position from the duplex terminus (**V**), the spin label bound fully at −30 °C. However, the data recorded at −20 °C shows that the abasic site needs to be at least at the fourth position from the duplex end (**VI**) to achieve full binding.

To investigate the binding efficiency of **Ġ** as a function of the identity of the base pairs immediately flanking the abasic site, a series of sixteen 14-mer RNA duplexes, with all possible combinations of the flanking bases, were prepared and incubated with **Ġ**. Visual inspection of the EPR spectra (see the Supporting Information, Figure S2) revealed relatively minor variations in the extent of binding between the flanking sequences. The binding was quantified by determining the dissociation constant (K_d) at 20 °C for all the flanking sequences, which showed a variation of K_d within a factor of two (see the Supporting Information, Figure S3). For comparison, up to 15-fold difference in the K_d was observed between flanking sequences for binding of the spin label **ç** to abasic sites in DNA duplexes.[16b] For a given base at the 5′-side of the abasic site, the highest affinity for **Ġ** was observed for a U at the 3′-side.

Conclusions

We have demonstrated that readily synthesized purine-derived nitroxide spin labels can be used for noncovalent spin-labeling

© 2018 Wiley-VCH Verlag GmbH & Co. KGaA, Weinheim

of abasic sites in nucleic acid duplexes, in particular RNA–RNA duplexes. Specifically, isoindoline-derived spin labels **3**, **5**, and **Ǵ** are superior for noncovalent spin-labeling when compared with the TEMPO-derived spin labels **2**, **4**, and **6**. The adenine derivative **5** and the guanine-nitroxide conjugate **Ǵ** bound efficiently to an abasic site of DNA duplexes and showed full binding to RNA duplexes. For all spin labels, the highest extent of binding was observed when the orphan base offered the possibility of Watson–Crick pairing; that is, when the adenine derivatives bound to T (DNA) or U (RNA) or the guanine derivatives to C. This indicates that hydrogen bonding is a significant contributor to spin-label binding. The adenine spin label **5** showed full binding to an abasic site of an RNA duplex opposite U and complements **Ǵ** as a spin label, which pairs with C. It was also demonstrated that **Ǵ** binds efficiently to abasic sites of DNA–RNA hybrids. Only a minor flanking-sequence effect was observed upon binding of **Ǵ** to an abasic site in RNA–RNA duplexes. Thus, spin labels **Ǵ** and **5** are promising spin labels for structural studies of RNA and its complexes with macromolecules.

Experimental Section

General materials and methods

All reagents were purchased from Sigma–Aldrich and were used without further purification. Dichloromethane and acetonitrile were dried over calcium hydride and freshly distilled before use. Thin-layer chromatography (TLC) was performed using glass plates pre-coated with silica gel (0.25 mm, F-25, Silicycle) and compounds were visualized under UV light. Column chromatography was performed using 230–400 mesh silica gel (Silicycle). ^{1}H NMR spectra were recorded with a Bruker Avance 400 MHz spectrometer. Chemical shifts are reported in parts per million (ppm) relative to the partially deuterated NMR solvent [D_6]DMSO (2.50 ppm). Nitroxide radicals show significant broadening in NMR spectra and loss of NMR signals due to their paramagnetic nature[27] and, therefore, those spectra are not reported. The EPR spectra of the radicals are shown in the Supporting Information. Mass spectrometric analyses were performed with an HRMS-ESI (Bruker, MicroTOF-Q) in positive ion mode. All EPR data were recorded in a phosphate buffer (10 mM $NaHPO_4$, 100 mM NaCl, 0.1 mM Na_2EDTA; pH 7) containing 30% ethylene glycol and 2% DMSO.

General procedure for the syntheses of spin labels 2–5

6-Chloropurine **7** or **10** (0.29 mmol) and nitroxide radical **8** or **9** (0.29 mmol) were added to a solution of *n*BuOH (4 mL) and Et_3N (0.88 mmol). The reaction mixture was heated at 120 °C for 16 h, cooled to RT and the solvent was evaporated in vacuo. The crude product was purified by flash column chromatography (silica gel) using a gradient elution (CH_2Cl_2/30% NH_3 in MeOH; 100:0 to 90:10) to give compounds **2**–**5** as pale-yellow solids.

Compound 2: Yield: 20 mg (22%); R_f = 0.22 (CH_2Cl_2/MeOH 9:1); HRMS-ESI: *m/z* calcd for $C_{14}H_{22}N_7O$ $[M+H]^+$ 305.1959; found: 305.1950.

Compound 3: Yield: 24 mg (25%); R_f = 0.25 (CH_2Cl_2/MeOH 9:1); HRMS-ESI: *m/z* calcd for $C_{17}H_{20}N_7O$ $[M+H]^+$ 339.1808; found: 339.1783.

Compound 4: Yield: 15 mg (16%); R_f = 0.28 (CH_2Cl_2/MeOH 9:1); HRMS-ESI: *m/z* calcd for $C_{17}H_{20}N_7O$ $[M+H]^+$ 290.1849; found: 290.1850.

Compound 5: Yield: 30 mg (29%); R_f = 0.28 (CH_2Cl_2/MeOH 9:1); HRMS-ESI: *m/z* calcd for $C_{17}H_{19}N_6O$ $[M+H]^+$ 324.1693; found: 324.1674.

Compound 11: Compound **7** (100 mg, 0.41 mmol) was added to 50% aqueous tetrafluoroboric acid (10 mL) and the solution was stirred at −20 °C for 15 min, followed by addition of aqueous sodium nitrite (2 mL, 1.5 M). The reaction mixture was stirred for 1 h at −10 °C, followed by neutralization with a satd. solution of sodium carbonate at 10 °C. The precipitate was filtered off and washed with cold water (10 mL) and dried in vacuo to give **11** (50 mg, 50%) as a pale-yellow solid. R_f = 0.62 (CH_2Cl_2/MeOH 9:1); ^{1}H NMR (400 MHz, [D_6]DMSO): δ = 13.64 (s, 1H), 8.41 (s, 1H), 7.55 (m, 2H), 7.44 (m, 3H), 5.60 ppm (s, 2H); ^{19}F NMR (400 MHz, [D_6]DMSO): δ = −53.08 ppm; HRMS-ESI: *m/z* calcd for $C_{12}H_9FN_4O$ $[M+Na]^+$ 267.0653; found: 267.0650.

Compound 12: Compound **11** (10 mg, 0.04 mmol) and 4-amino-TEMPO (**8**) (8.5 mg, 0.05 mmol) were added to a solution of anhydrous DMF (0.7 mL) and Et_3N (18 μL, 0.12 mmol) and heated at 100 °C for 12 h. The reaction mixture was cooled to RT and the solvent was evaporated in vacuo. The crude material was purified by flash column chromatography (silica gel) using a gradient elution (CH_2Cl_2: 30% NH_3 in MeOH; 100:0 to 90:10) to give **12** (4 mg, 24%) as a pale-yellow solid. R_f = 0.32 (CH_2Cl_2/MeOH 9:1); HRMS-ESI: *m/z* calcd for $C_{12}H_9FN_4O$ $[M+H]^+$ 396.2268; found: 396.2261.

Compound 6: To a solution of compound **12** (12 mg, 0.02 mmol) in MeOH (5 mL) was added 10% Pd/C (1 mg) under argon. The mixture was stirred under H_2 gas (55 psi) at 22 °C for 16 h, the mixture was filtered through a pad of Celite and the filtrate was concentrated in vacuo to give **6** (7 mg, 80%). R_f = 0.32 (CH_2Cl_2/MeOH 9:1); HRMS-ESI: *m/z* calcd for $C_{14}H_{21}N_6O_2$ $[M+H]^+$ 306.1799; found: 306.1792.

DNA and RNA synthesis and purification

Phosphoramidites, CPG columns, 5-benzylthiotetrazole and acetonitrile for oligomer synthesis were purchased from ChemGenes Corp., USA. All other required reagents and solvents were purchased from Sigma–Aldrich. Unmodified oligonucleotides and oligonucleotides containing abasic sites were synthesized with an automated ASM800 DNA synthesizer (Biosset, Russia) using a trityl-off protocol and phosphoramidites with standard protecting groups on 1.0 μmole scale (1000 Å CPG columns). The DNAs were deprotected from solid support using 33% aqueous ammonia solution at 55 °C for 8 h, whereas the general deprotection for RNAs was done using 1:1 solution (2 mL) of CH_3NH_2 (8 M in EtOH) and NH_3 (33% w/w in H_2O) at 65 °C for 45 min. The solvent was removed in vacuo and the TBDMS-protecting groups were removed by incubation in $NEt_3{\cdot}3HF$ (600 μL) for 90 min at 55 °C in DMF (200 μL), followed by addition of water (200 μL) and precipitation in 1-butanol. The oligonucleotides were purified by 20% denaturing polyacrylamide gel electrophoresis. The oligonucleotides were visualized under UV light and the bands were excised from the gel, crushed, and extracted from the gel matrix with a Tris buffer (250 mM NaCl, 10 mM Tris, 1 mM Na_2EDTA, pH 7.5). The extracts were filtered through 0.45 μm, 25 mm diameter GD/X syringe filters (Whatman, USA) and desalted using Sep-Pak cartridges (Waters, USA), according to the manufacturer's instructions. After removing the solvent in vacuo, the oligomers were dissolved in deionized and sterilized water (200 μL). Oligonucleotides were quantified using Beer's law and measurements of absorbance at 260 nm, using extinction coef-

© 2018 Wiley-VCH Verlag GmbH & Co. KGaA, Weinheim

ficients determined by using the WinLab oligonucleotide calculator (V2.85.04, PerkinElmer).

EPR measurements

Solutions for CW-EPR experiments were prepared by mixing aliquots of stock solutions of a single-stranded oligomer containing an abasic site, its complementary strand, and the spin label (1:1.2:0.5). The solvent was evaporated in vacuo and the resulting residue was dissolved in phosphate buffer (10 μL; 10 mM $NaHPO_4$, 100 mM NaCl, 0.1 mM Na_2EDTA, pH 7.0) and annealed: 90 °C for 2 min, 60 °C for 5 min, 50 °C for 5 min, 22 °C for 15 min and dried using a SpeedVac. The residue was dissolved in aqueous 30% ethylene glycol (10 μL) containing 2% DMSO and placed in a 50 μL quartz capillary (BLAUBRAND intraMARK) (final concentration of nucleic acid duplex 200 μM). The EPR spectra were recorded using 100–200 scans with a MiniScope MS200 (Magnettech Germany) spectrometer (100 kHz modulation frequency, 1.0 G modulation amplitude and 2.0 mW microwave power). Magnettech temperature controller M01(±0.5 °C) was used as a temperature regulator.

Acknowledgements

This research work was supported by the Icelandic Research Fund (141062-051). N.R.K. gratefully acknowledges the University of Iceland Research Fund for providing the doctoral research fellowship. We thank Dr. Subham Saha for critically reading this manuscript and Dr. S. Jonsdottir for assistance in collecting analytic data for structural characterization of the compounds.

Conflict of interest

The authors declare no conflict of interest.

Keywords: DNA/RNA · EPR spectroscopy · noncovalent interactions · spin labels · structure elucidation

[1] a) O. Schiemann, T. F. Prisner, *Q. Rev. Biophys.* **2007**, *40*, 1–53; b) G. Z. Sowa, P. Z. Qin, *Prog. Nucleic Acid Res. Mol. Biol.* **2008**, *82*, 147–197; c) L. Hunsicker-Wang, M. Vogt, V. J. Derose, *Methods Enzymol.* **2009**, *468*, 335–367; d) X. Zhang, P. Cekan, S. T. Sigurdsson, P. Z. Qin, *Methods Enzymol.* **2009**, *469*, 303–328; e) G. W. Reginsson, O. Schiemann, *Biochem. Soc. Trans.* **2011**, *39*, 128–129; f) I. Krstić, B. Endeward, D. Margraf, A. Marko, T. F. Prisner, in *EPR Spectroscopy*, Springer, **2011**, pp. 159–198; g) Y. Ding, P. Nguyen, N. Tangprasertchai, C. Reyes, X. Zhang, P. Qin, *Electron Paramagn. Reson.* **2014**, *24*, 122–147.

[2] a) H.-J. Steinhoff, *Front. Biosci.* **2002**, *7*, c97–110; b) G. Jeschke, *Annu. Rev. Phys. Chem.* **2012**, *63*, 419–446; c) J. P. Klare, *Biol. chem.* **2013**, *394*, 1281–1300; d) E. R. Georgieva, *Nanotechnol. Rev.* **2017**, *6*, 75–92.

[3] a) W. L. Hubbell, D. S. Cafiso, C. Altenbach, *Nat. Struct. Mol. Biol.* **2000**, *7*, 735–739; b) P. Z. Qin, J. Iseri, A. Oki, *Biochem. Biophys. Res. Commun.* **2006**, *343*, 117–124; c) P. Nguyen, P. Z. Qin, *Wiley Interdiscip. Rev.: RNA* **2012**, *3*, 62–72.

[4] a) J. Macosko, M. Pio, I. Tinoco, Y.-K. Shin, *RNA* **1999**, *5*, 1158–1166; b) N.-K. Kim, A. Murali, V. J. DeRose, *Chem. Biol.* **2004**, *11*, 939–948; c) H.-J. Steinhoff, *Biol. Chem.* **2004**, *385*, 913–920.

[5] a) P. P. Borbat, J. H. Davis, S. E. Butcher, J. H. Freed, *J. Am. Chem. Soc.* **2004**, *126*, 7746–7747; b) G. Jeschke, Y. Polyhach, *Phys. Chem. Chem. Phys.* **2007**, *9*, 1895–1910; c) G. W. Reginsson, O. Schiemann, *Biochem. J.* **2011**, *434*, 353–363; d) Z. Yang, Y. Liu, P. Borbat, J. L. Zweier, J. H. Freed, W. L. Hubbell, *J. Am. Chem. Soc.* **2012**, *134*, 9950–9952; e) O. Duss, M. Yulikov, G. Jeschke, F. H. Allain, *Nat. Commun.* **2014**, *5*, 3669; f) D. Goldfarb, in *Structural Information from Spin-Labels and Intrinsic Paramagnetic Centres in the Biosciences*, Springer **2012**, pp. 163–204.

[6] a) A. Marko, V. Denysenkov, D. Margraf, P. Cekan, O. Schiemann, S. T. Sigurdsson, T. F. Prisner, *J. Am. Chem. Soc.* **2011**, *133*, 13375–13379; b) T. F. Prisner, A. Marko, S. T. Sigurdsson, *J. Magn. Reson.* **2015**, *252*, 187–198; c) B. Endeward, A. Marko, V. Denysenkov, S. T. Sigurdsson, T. F. Prisner, *Methods Enzymol.* **2015**, *564*, 403–425; d) C. M. Grytz, A. Marko, P. Cekan, S. T. Sigurdsson, T. F. Prisner, *Phys. Chem. Chem. Phys.* **2016**, *18*, 2993–3002; e) C. M. Grytz, S. Kazemi, A. Marko, P. Cekan, P. Güntert, S. T. Sigurdsson, T. F. Prisner, *Phys. Chem. Chem. Phys.* **2017**, *19*, 29801–29811.

[7] a) S. A. Shelke, S. T. Sigurdsson, *Site-Directed Nitroxide Spin Labeling of Biopolymers*, Springer, **2011**, pp. 121–162; b) S. A. Shelke, S. T. Sigurdsson, *Eur. J. Org. Chem.* **2012**, 2291–2301; c) S. A. Shelke, S. T. Sigurdsson, in *Modified Nucleic Acids*, Springer, **2016**, pp. 159–187.

[8] a) A. Spaltenstein, B. H. Robinson, P. B. Hopkins, *J. Am. Chem. Soc.* **1988**, *110*, 1299–1301; b) N. Barhate, P. Cekan, A. P. Massey, S. T. Sigurdsson, *Angew. Chem. Int. Ed.* **2007**, *46*, 2655–2658; *Angew. Chem.* **2007**, *119*, 2709–2712; c) C. Höbartner, G. Sicoli, F. Wachowius, D. B. Gophane, S. T. Sigurdsson, *J. Org. Chem.* **2012**, *77*, 7749–7754; d) D. B. Gophane, S. T. Sigurdsson, *Chem. Commun.* **2013**, *49*, 999–1001.

[9] O. Schiemann, N. Piton, J. Plackmeyer, B. E. Bode, T. F. Prisner, J. W. Engels, *Nat. Protoc.* **2007**, *2*, 904–923.

[10] a) N. Piton, Y. Mu, G. Stock, T. F. Prisner, O. Schiemann, J. W. Engels, *Nucleic Acids Res.* **2007**, *35*, 3128–3143; b) P. Cekan, A. L. Smith, N. Barhate, B. H. Robinson, S. T. Sigurdsson, *Nucleic Acids Res.* **2008**, *36*, 5946–5954.

[11] a) P. Z. Qin, K. Hideg, J. Feigon, W. L. Hubbell, *Biochemistry* **2003**, *42*, 6772–6783; b) T. E. Edwards, S. T. Sigurdsson, *Nat. Protoc.* **2007**, *2*, 1954–1962; c) U. Jakobsen, S. A. Shelke, S. Vogel, S. T. Sigurdsson, *J. Am. Chem. Soc.* **2010**, *132*, 10424–10428; d) G. Sicoli, F. Wachowius, M. Bennati, C. Höbartner, *Angew. Chem. Int. Ed.* **2010**, *49*, 6443–6447; *Angew. Chem.* **2010**, *122*, 6588–6592; e) S. Saha, A. P. Jagtap, S. T. Sigurdsson, *Chem. Commun.* **2015**, *51*, 13142–13145; f) M. M. Haugland, A. H. El-Sagheer, R. J. Porter, J. Peña, T. Brown, E. A. Anderson, J. E. Lovett, *J. Am. Chem. Soc.* **2016**, *138*, 9069–9072; g) K. Halbmair, J. Seikowski, I. Tkach, C. Höbartner, D. Sezer, M. Bennati, *Chem. Sci.* **2016**, *7*, 3172–3180.

[12] a) B. K. Sinha, C. F. Chignell, *Life Sci.* **1975**, *17*, 1829–1836; b) S.-J. Hong, L. H. Piette, *Cancer Res.* **1976**, *36*, 1159–1171; c) S.-J. Hong, L. Piette, *Arch. Biochem. Biophys.* **1978**, *185*, 307–315; d) I. Hurley, P. Osei-Gyimah, S. Archer, C. Scholes, L. Lerman, *Biochemistry* **1982**, *21*, 4999–5009; e) M. F. Ottaviani, N. D. Ghatlia, S. H. Bossmann, J. K. Barton, H. Duerr, N. J. Turro, *J. Am. Chem. Soc.* **1992**, *114*, 8946–8952; f) P. B. Dervan, *Bioorg. Med. Chem.* **2001**, *9*, 2215–2235.

[13] a) H. Atsumi, K. Maekawa, S. Nakazawa, D. Shiomi, K. Sato, M. Kitagawa, T. Takui, K. Nakatani, *Chem. Lett.* **2010**, *39*, 556–557; b) H. Atsumi, S. Nakazawa, C. Dohno, K. Sato, T. Takui, K. Nakatani, *Chem. Commun.* **2013**, *49*, 6370–6372.

[14] a) K. Yoshimoto, S. Nishizawa, M. Minagawa, N. Teramae, *J. Am. Chem. Soc.* **2003**, *125*, 8982–8983; b) B. Rajendar, S. Nishizawa, N. Teramae, *Org. Biomol. Chem.* **2008**, *6*, 670–673.

[15] a) P. Belmont, C. Chapelle, M. Demeunynck, J. Michon, P. Michon, J. Lhomme, *Bioorg. Med. Chem. Lett.* **1998**, *8*, 669–674; b) F. Thomas, J. Michon, J. Lhomme, *Biochemistry* **1999**, *38*, 1930–1937.

[16] a) S. A. Shelke, S. T. Sigurdsson, *Angew. Chem. Int. Ed.* **2010**, *49*, 7984–7986; *Angew. Chem.* **2010**, *122*, 8156–8158; b) S. A. Shelke, S. T. Sigurdsson, *Nucleic Acids Res.* **2012**, *40*, 3732–3740; c) S. A. Shelke, G. B. Sandholt, S. T. Sigurdsson, *Org. Biomol. Chem.* **2014**, *12*, 7366–7374.

[17] G. W. Reginsson, S. A. Shelke, C. Rouillon, M. F. White, S. T. Sigurdsson, O. Schiemann, *Nucleic Acids Res.* **2013**, *41*, e11.

[18] N. R. Kamble, M. Gränz, T. F. Prisner, S. T. Sigurdsson, *Chem. Commun.* **2016**, *52*, 14442–14445.

[19] D. Reid, S. Bottle, *Chem. Commun.* **1998**, 1907–1908.

[20] R. C. Moschel, A. E. Pegg, M. E. Dolan, M.-Y. Chae, US005958932A, **1999**.

[21] I. R. Hardcastle, C. E. Arris, J. Bentley, F. T. Boyle, Y. Chen, N. J. Curtin, J. A. Endicott, A. E. Gibson, B. T. Golding, R. J. Griffin, *J. Med. Chem.* **2004**, *47*, 3710–3722.

[22] a) F. Wyers, A. Sentenac, P. Fromageot, *Eur. J. Biochem.* **1973**, *35*, 270–281; b) I. Sidorenkov, N. Komissarova, M. Kashlev, *Mol. Cell* **1998**, *2*, 55–64; c) E. Zamaratski, P. Pradeepkumar, J. Chattopadhyaya, *J. Biochem. Biophys. Methods* **2001**, *48*, 189–208; d) M. Nowotny, S. A. Gaidamakov, R. J. Crouch, W. Yang, *Cell* **2005**, *121*, 1005–1016; e) A. Rich, *J. Biol.*

© 2018 Wiley-VCH Verlag GmbH & Co. KGaA, Weinheim

Chem. **2006**, *281*, 7693 – 7696; f) C. Ohle, R. Tesorero, G. Schermann, N. Dobrev, I. Sinning, T. Fischer, *Cell* **2016**, *167*, 1001 – 1013.

[23] T. Aboul-Fadl, *Curr. Med. Chem.* **2005**, *12*, 2193 – 2214.

[24] a) O. Y. Fedoroff, M. Salazar, B. R. Reid, *J. Mol. Biol.* **1993**, *233*, 509 – 523; b) B. M. Znosko, T. W. Barnes, T. R. Krugh, D. H. Turner, *J. Am. Chem. Soc.* **2003**, *125*, 6090 – 6097.

[25] a) G. L. Conn, T. Brown, G. A. Leonard, *Nucleic Acids Res.* **1999**, *27*, 555 – 561; b) Y. Xiong, M. Sundaralingam, *Nucleic Acids Res.* **2000**, *28*, 2171 – 2176; c) M. L. Kopka, L. Lavelle, G. W. Han, H.-L. Ng, R. E. Dickerson, *J. Mol. Biol.* **2003**, *334*, 653 – 665; d) G. W. Han, M. L. Kopka, D. Langs, M. R. Sawaya, R. E. Dickerson, *Proc. Natl. Acad. Sci. USA* **2003**, *100*, 9214 – 9219.

[26] D. Andreatta, S. Sen, J. L. Pérez Lustres, S. A. Kovalenko, N. P. Ernsting, C. J. Murphy, R. S. Coleman, M. A. Berg, *J. Am. Chem. Soc.* **2006**, *128*, 6885 – 6892.

[27] a) T. D. Lee, J. F. Keana, *J. Org. Chem.* **1975**, *40*, 3145 – 3147; b) Y. Li, X. Lei, X. Li, R. G. Lawler, Y. Murata, K. Komatsu, N. J. Turro, *Chem. Commun.* **2011**, *47*, 12527 – 12529.

Manuscript received: November 14, 2017
Version of record online: ■■ ■■, 0000

© 2018 Wiley-VCH Verlag GmbH & Co. KGaA, Weinheim

FULL PAPER

Binding without bonding: Isoindoline-derived purine spin-labels bind efficiently to abasic sites of duplex DNA and RNA when they can form hydrogen bonds to the orphan base on the opposing strand; the adenine-derived spin label **5** pairs with uracil (or thymine) and the guanine-derivative **Ǵ** pairs with cytosine. The latter also binds to abasic sites in DNA–RNA hybrid duplexes and shows a minimal flanking-sequence effect upon binding to abasic sites in RNA.

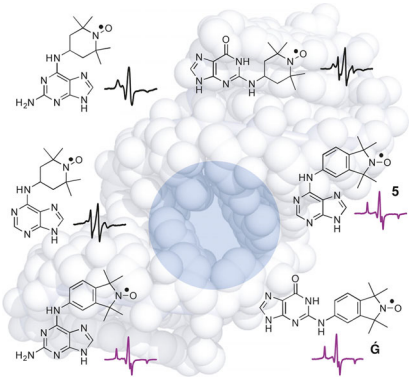

Spin Labels

*N. R. Kamble, S. Th. Sigurdsson**

■■ – ■■

Purine-Derived Nitroxides for Noncovalent Spin-Labeling of Abasic Sites in Duplex Nucleic Acids

© 2018 Wiley-VCH Verlag GmbH & Co. KGaA, Weinheim